OPEN ACCESS
Unmanned Systems (2027) 1–17

DOI: 10.1142/S2301385027500646

UNMANNED SYSTEMS
https://www.worldscientific.com/worldscinet/us

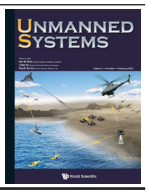

Stabilizing Acceleration Controllers for Multiple Planar Wheelchair Robots in Constrained Environment

Bouatake Hedstrom [*], Rishi Autar [*], Veisinia Vatikani [*], Sushita Sharma [*], Ronal P. Chand [†], Sandeep A. Kumar [*,‡]

[*]*School of Information Technology, Engineering, Mathematics and Physics, The University of the South Pacific, Fiji*

[†]*School of Mathematical and Computing Sciences, Fiji National University, Fiji*

The integration of robotics into assistive technology is gaining significant attention in research. One area that has seen a dramatic increase in usage is the wheelchair for people with disabilities. This paper introduces a set of novel acceleration-based controllers designed for navigating multiple planar wheelchair robots in constrained environments. These wheelchair controllers are derived from the total potential constructed using Lyapunov-based Control Scheme (LbCS), which is captured under the classical Artificial Potential Field (APF) method. The effectiveness of the proposed controllers was validated numerically and through computer simulations using Wolfram Mathematica 13.3 software. The results demonstrate that the acceleration-based controllers successfully navigate the wheelchair robots to their final configuration space in complex, constrained environments. They exhibit robust obstacle and collision avoidance and adhere to system restrictions, which are due to the motion control planning via LbCS. The proposed controllers show high adaptability, making them suitable for various assistive and collaborative robotic applications.

Keywords: Assistive technology; wheelchair; motion planning; APF; acceleration-based controllers.

1. Introduction

Over centuries, there has been a need for Assistive Technologies (AT) to aid People with Special Needs (PSN) or physical disabilities. The ATs have been designed and crafted to simulate either some form of animal or human behaviour to assist PSNs in mobility, vision, hearing and other human functions that may have been challenged or lost due to hereditary traits, accidents, poor health or ageing [1]. Industry 1.0 describes the first industrial revolution in the 1700s of the use of simple handicrafts to mechanical systems to enhance the productivity and functionality of products as evidenced in the transition of AT [2]. The ATs have evolved over the years in many forms, using various approaches to suit all types of impairments and enhance the livelihoods of those living with disabilities. Some instances, where AT has been incorporated successfully, include an exosuit for assisting elbow movements and hand grasping in daily activities for those that have lost limb usage [3], hearing aids for those with severe or profound hearing loss [4], smart glasses to aid those with visual impairments [5] and caregiving assistive

Received 10 February 2025; Accepted 19 January 2026; Published 10 February 2026. This paper was recommended for publication in its revised from by editorial board member, Wei Liu.
Email addresses: [‡]*sandeep.kumar@usp.ac.fj*
[‡]Corresponding author.

robots for individuals with health or ageing problems [6]. The integration of robotics in AT is currently one of the main research focuses as, according to the International Organisation for Standardisation (ISO), "... robots are automatic, position-controlled, multi-functioned manipulators..." [7] that have the capability to handle a variety of materials, components, tools, and specialized equipment via programmable automation in order to execute specified tasks, and its use in AT is extensively broadening the horizon for PSNs, as proposed by Martinez-Martin *et al.* [8] where they developed cognitive and robotic assistants for elderly care, the use of educational robots to assist students with visual impairments [9] and the development of humanoid robots to assist children with hearing disabilities [10]. The developments in AT described by Xiloyannis *et al.*, [3] Busaeed *et al.* [5] and Arthanat *et al.* [6] were made possible after the evolution of Industry 3.0, which was also known as the digital revolution whereby simple automation was developed through the use of computers and programmable logic controllers and thus ignited the inception of autonomous control through computer technology [11].

Meanwhile, an AT, that is widely used, is the wheelchair, which aids in mobility and generally enhances the user's interaction with its environment despite the loss of ability to walk. Recent studies have shown that many approaches have been used in developing smart, semi-autonomous, and autonomous wheelchairs to provide optimum assistance to the user. For the wheelchair to get into motion, a variety of methodologies have been presented in the literature, ranging from the use of Electromyography (EMG) whereby signals are detected from the motion of neck and arm muscles [12], Electrooculogram (EOG) which uses signals from eye movements [13], voice control where an adaptive neuro-fuzzy controller was utilized for producing the necessary real-time control signals to activate the wheelchair's motors [14] and multi-controlled semi-autonomous wheelchairs whereby the wheelchair is controlled through the combination of joystick [15], hand gesture [16], voice [17], the use of tongue gesture to access a computer and drive a wheelchair [18], android application for speed and direction control of the wheelchair [19]. The majority of the proposed designs in literature were mostly conjured on the basic idea of some to no human aid needed to ensure full independence of the wheelchair user [12–19]. The aspirations of wheelchair designers to craft and manufacture a product that requires no human control has led to the proposal of various motion planning approaches.

The need for autonomous wheelchairs that require no human interaction materialised in order to address cases of severe impairment where PSNs have no remaining ability to enable their full independence from wheelchair control. In 2021, Kumar *et al.* developed velocity controllers using the Lyapunov-based Control Scheme (LbCS) technique for motion planning of a wheelchair in an obstacle-ridden environment [20], but the comfort of the user may be compromised as the velocity controllers caused sharp changes in the wheelchair motion resulting in jerky movements. Furthermore, in 2022, Ryu *et al.* incorporated the use of artificial intelligence to control a wheelchair [21]. However, in the literature, the development of acceleration controllers for an autonomous wheelchair, which will allow no human interaction for mobility as well as ensure the comfort of the user, has not been studied.

This paper provides a solution to the *findpath problem* for $n \in \mathbb{N}$ planar wheelchair robots with the requirement that the individual robots are converging to their respective targets and adhere to system limitations. This is achieved by deriving a set of novel two dimensional nonlinear stabilizing continuous acceleration controllers for $n \in \mathbb{N}$ planar wheelchair robots to navigate a cluttered environment with stationary disk, elliptic and line segment obstacles. The controllers are derived from a total potential, which is developed utilising the LbCS, a modified classical APF methodology. The total potential will be a sum attractive and repulsive potential fields. An attraction function will be developed for target convergence and repulsive functions will be developed for obstacle and collision avoidances and for adherence to system restrictions and limitations. These functions will later be used to form the attractive and repulsive potential fields, which are going to be part of the total potential called a Lyapunov function. Some notable challenges in developing the controllers of the wheelchair robots using LbCS are

- The wheelchair robot is a nonholonomic system with nonintegrable motion constraints, requiring careful handling of its kinematic structure.
- The system is underactuated, and mapping desired accelerations to admissible control inputs consistent with the nonholonomic constraints can lead to singularities or infeasibility.
- Constructing a Lyapunov function that captures both position and velocity dynamics while ensuring asymptotic stability of the closed-loop system is nontrivial.
- Input saturation due to actuator limits complicates the design, as acceleration-based inputs can easily exceed physical capabilities if not properly bounded.
- Environment complexity gives rise to local minima issues, conservative trajectories, and difficulties in designing an appropriate Lyapunov function.
- Scalability gives rise to computational burden.

The advantage of using LbCS is the simplicity in the design of continuous nonlinear controllers. It is also relatively easier to capture the mechanical constraints in the controllers designed using LbCS when compared to the other

motion planning control schemes present n the literature. Scalability is not ensured as any increase in the number of wheelchairs or obstacles would increase environment complexity demanding greater computing resources. However, the advancing IT industry producing increasing processing power, memory, and computing storage devices with decreasing prices for them could play a role in diminishing the scaling impact.

The major contribution of this paper is the design of a set of novel two dimensional nonlinear stabilizing continuous acceleration controllers for $n \in \mathbb{N}$ planar wheelchair robots to navigate a cluttered environment with stationary disk, elliptic and line segment obstacles. This contrasts with previous LbCS approache primarily employing velocity controllers [20], and aims to provide inherently smoother motion, enhanced user comfort, and in applied situations, potentially reduced mechanical wear. The autonomous navigation and coordination of $n \in \mathbb{N}$ planar wheelchair robots within a shared constrained space validates robust inter-agent collision avoidance scheme of LbCS. The system presented is an advancement over study presented by Kumar *et al.* in 2021, where a single planar wheelchair robot was navigated in only disk obstacle cluttered environment [20]. Collectively, these contributions offer a significant advancement toward fully autonomous, comfortable, and safe mobility solutions for individuals with severe impairments using multiple cooperating wheelchairs navigating complex static environments.

This paper is arranged as follows. Section 2 provides a literature review that will compare and highlight other works similar to our research, followed by Sec. 3, which explores the LbCS, and then followed by Sec. 4, which describes the Model of a Nonholonomic Wheelchair. Section 5 describes the problem statement followed by the design of acceleration-based controllers of multiple wheelchair robots in Sec. 6. Section 7 will provide simulations of the acceleration controllers in a hypothetical workspace, which is followed by Sec. 8, which provides a discussion of results and any limitations encountered. Finally, Sec. 9 gives the conclusion with the inclusion of future works.

2. Literature Review

The development of autonomous wheelchair robots has gained significant momentum in recent years, driven by advancements in robotics, Artificial Intelligence (AI), and sensor technology. The innovations in the development of autonomous wheelchair robots aim to enhance the mobility and independence of individuals with disabilities. This literature review examines key works and technological advancements in the field, comparing various approaches and highlighting their contributions and limitations.

The manual wheelchair was first invented in 1783 by John Dawson to transport the sick to the healing waters of Bath, England [22]. This manual wheelchair evolved over the centuries with improved design and innovation for user comfort as well as adaptability to the environment [23]. However, the manual wheelchair either required another person to move it or the user themselves to mobilise the wheelchair, which became a major drawback as it put limitations on user independence as well as added more burden to the user trying to propel themselves rather than assist them [24].

The limitation of the manual wheelchair gave rise to the introduction of the electric wheelchair, which was first invented by George Klein in 1953 to assist World War II veterans [25]. Other researchers improved his work over the years in their quest to enhance wheelchair use. In 2006, Dicianno *et al.* proposed the use of joysticks to propel the wheelchair [15], which gave independence and comfort to the user. Similarly, in 2020, Abdulghani *et al.* developed a wheelchair that was voice-controlled [14] and likewise in the same year Rakasena *et al.* [12] developed a wheelchair that was controlled by elbow and hand muscles. However, despite their modern and creative propulsion designs, they still had limitations for users with no remaining ability to control the wheelchair. This limitation then gave rise to the need for an autonomous wheelchair that required no human interaction for control.

A critical aspect of autonomous wheelchairs is their ability to navigate complex environments safely. Many studies focus on integrating sensors for obstacle detection and path planning. Tang *et al.* developed a system incorporating LIDAR and ultrasonic sensors to create real-time maps, enabling the wheelchair to navigate indoor environments autonomously [26]. Their approach emphasized the importance of sensor fusion for accurate environment perception. In the same year, Morales *et al.* [27] developed a predictive control algorithm that anticipates the user's desired destination based on past behaviour and current context. It considered the passenger's comfort perception and planned a path that best suited the user's comfort. This predictive approach reduced the need for constant user input, improving user experience. However, they identified challenges related to the algorithm's adaptability to sudden changes in the environment.

Effective human–robot interaction is crucial for the usability of smart wheelchairs. Coelho *et al.* introduced a multi-modal interface that integrates voice commands, touch screens, and joystick controls to manoeuvre wheelchair robots, which integrated the concept of AI with robotics [28]. Their system allowed users to switch between control modes seamlessly, enhancing the wheelchair's adaptability to different user preferences and needs. Later in 2021, Kim *et al.* investigated the use of Brain-Computer Interfaces (BCIs) for

controlling autonomous wheelchairs [29]. Their research demonstrated that BCIs could provide a non-invasive and efficient means of control for users with severe motor impairments. However, they noted that the technology's reliability and accuracy needed improvement for practical application.

Moreover, Farheen explored the use of vision-based systems combined with AI for obstacle avoidance [30] by employing deep learning algorithms to interpret visual data, allowing the wheelchair to recognise and react to dynamic obstacles, such as pedestrians. The later study highlighted the potential of combining computer vision with machine learning for robust autonomous navigation. Most recently, Sharma presented an innovative approach to assistive robotics by introducing a robotic dog to guide a rehabilitation wheelchair robot in highly constrained environments. Utilising nonlinear control laws derived from a Lyapunov-based control scheme, the robotic dog leads the wheelchair through obstacle-free paths, offering increased mobility for users with physical disabilities [31]. Beyond individual navigation, coordinating multiple autonomous agents, such as the wheelchairs considered in this work or other platforms like Autonomous Surface Vessels (ASVs) [32, 33] and Autonomous Underwater Vehicles (AUVs) [34], introduces significant challenges. These include managing interactions, handling model uncertainties and external disturbances, and respecting operational constraints. Recent research across these varied robotic domains has explored advanced control techniques to address such issues. For instance, strategies often combine formation, platoon, or tracking objectives with adaptive methods, such as various types of neural networks [32–34] or self-tuning algorithms based on system identification [35], to compensate for uncertainties and disturbances. Furthermore, Barrier Lyapunov Functions (BLFs), sometimes in asymmetric or time-varying forms, have been effectively utilized to enforce state or output constraints, including operational limits or sensor field-of-view restrictions [32–34], thereby ensuring system safety and integrity during complex maneuvers, with some approaches achieving fixed-time error convergence [33].

It is quite evident from the literature that most of the wheelchair systems needed at least some form of human interaction, which would be a great disadvantage for a PSN who has lost all forms of ability such as brain function, motor, and vision and cannot control the wheelchair. Therefore, there is a need for further research to develop an autonomous wheelchair that requires minimum to no input from its user for navigation and routine activities. This paper will propose autonomous acceleration-based controllers that will enable multiple wheelchairs to navigate constrained environments. To ensure effective mobile planning, LbCS will be employed as it is evident in the literature that LbCS is robust when it comes to obstacle and collision avoidance and incorporating system restrictions and limitations.

3. The Lyapunov-based Control Scheme

This research will use an artificial potential field method, the Lyapunov-based Control Scheme (LbCS). The LbCS collision avoidance method was first proposed by Stonier in 1983 whereby to ensure collision avoidance between two point masses moving toward their respective targets on a horizontal plane; a Lyapunov-like function was employed to derive analytical control laws for their planar motion [36]. However, the Lyapunov-like function initially devised by Stonier and later refined by Vanualailai *et al.* [37], had a notable limitation. It failed to meet the Lyapunov stability condition, which necessitates precise zeroing at the system's stable equilibrium points. In 1998, Ha and Vanualailai [38] enhanced Stonier's approach by introducing an auxiliary function that adhered to the sufficient conditions of Lyapunov's stability theorem. This improvement enabled the construction of a Lyapunov function applicable to multiple point-mass systems and planar robotic arms. Notably, their method only necessitates control parameters to govern trajectory direction, offering potential applications across various mechanical systems.

The LbCS method primarily develops the attraction and repulsion potential field functions, which make up the total potential for a Lyapunov function. The LbCS has been implemented with success for various applications in motion planning and collision avoidance for optimum solutions [31, 39–42]. The primary aim of the LbCS is the expansion of attractive and repulsive potential field functions from which consequently one can derive nonlinear velocity or acceleration controllers [43–45]. The LbCS is user-friendly in deriving controllers as they are straightforward, and the controllers are continuous, which are its advantages. There is an ease in the inclusion of any restrictions or parameters while deriving the mathematical functions. However, the main drawback for LbCS is the initiation of the local minima. In practical scenarios, continuity must be developed discretely before demonstrating its approach toward equilibrium.

Figure 1 demonstrates the effectiveness of the Lyapunov-based control scheme in guiding the robot through its workspace. Figure 1(a) depicts the robot's initial position at (10, 10), its target at (85, 100), and its trajectory (dashed line), successfully avoiding two randomly generated obstacles with a radius of 10, while reaching the final destination. Additionally, Fig. 1(b) shows a monotonically decreasing potential field from the initial position, which reaches zero at the target.

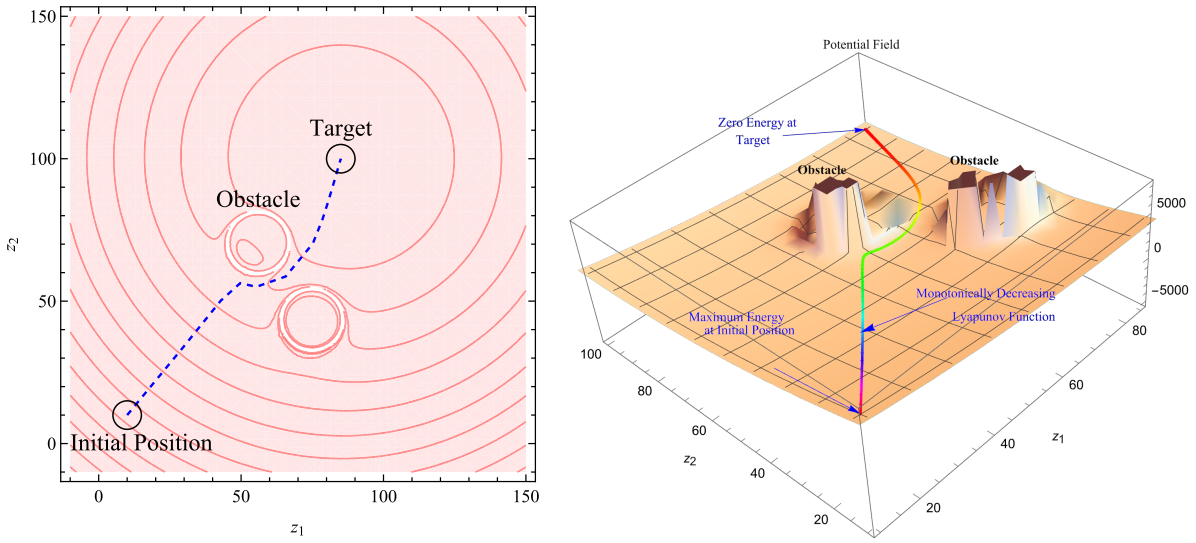

(a) (b)

Fig. 1. An illustration of the Lyapunov-based control scheme. (a) Contour plot and (b) 3D visualization.

3.1. *LbCS algorithmic workflow*

An algorithmic representation of the LbCS methodology for the motion planning of multiple wheelchair system is presented below.

(1) **System Modeling:** Define the kinematic model of the nonholonomic wheelchair robots, including their state variables and motion equations (as detailed in Sec. 4, Eq. (5)).
(2) **Define Objectives and Constraints:** Identify the primary goals (reaching designated targets τ_i) and constraints (avoiding stationary obstacles W_j, F_k, Q_p, inter-robot collisions H_{i_h}, and respecting velocity limits A_i, B_i).
(3) **Design Potential Functions:** For each objective and constraint, design corresponding potential functions. This includes target attraction functions (T_i, Eq. (7)), stationary obstacle avoidance functions ($W_{i_j}, F_{i_k}, Q_{i_p}$), inter-agent collision avoidance functions (H_{i_h}, Eq. (13)), and artificial potential functions for velocity limits (A_i, B_i). Auxiliary functions (G_i) are also introduced to ensure controllers vanish at the target (as detailed in Sec. 6.1).
(4) **Construct Lyapunov Function:** Combine these individual potential functions into a single, composite Lyapunov function candidate $L(\mathbf{x})$ (Eq. (17)). Positive weighting parameters ($\alpha_i, \beta_{i_k}, \gamma_{i_j}, \rho_{i_p}, \epsilon_{i_h}, \mu_i, \sigma_i$) are assigned to balance the influence of each component.
(5) **Derive Acceleration Controllers:** Calculate the time derivative of the Lyapunov function, $\dot{L}(\mathbf{x})$, along the system trajectories (5). Design the acceleration control inputs (u_{1_i}, u_{2_i}, Eq. (21)) such that $\dot{L}(\mathbf{x})$ is guaranteed to be negative semi-definite (≤ 0). This typically involves relating the control inputs to the negative gradient components of $L(\mathbf{x})$ (detailed in Sec. 6.2.1).
(6) **Stability Analysis:** Prove the asymptotic stability of the system under the derived controllers using Lyapunov theory and LaSalle's Invariance Principle (as shown in Sec. 6.2.2).
(7) **Simulation:** Implement the kinematic model (5) with the derived acceleration controllers (21) in a simulation environment using Mathematica 13.3 to validate performance of the derived controllers.

This step-by-step process forms the core methodology for achieving stable, autonomous navigation of multiple wheelchairs in constrained environments using LbCS. A visual representation of this workflow is provided in Fig. 2.

4. A Model of a Nonholonomic Wheelchair

Definition 4.1. The ith wheelchair with front castor wheels and driven by two back wheels is a disk with radius r_{v_i}, centre $(x_i, y_i) \in \mathbb{R}^2$ where $i \in \mathbb{N}$. It is described as the set

$$P = \{(Z_1, Z_2) \in \mathbb{R}^2 : (Z_1 - x_i)^2 + (Z_2 - y_i)^2 \leq r_{v_i}^2\}.$$

Figure 3 shows a wheelchair robot propelled by two back wheels with two front swivelling wheels. The two back wheels, each with a diameter of r, are positioned at opposite ends of a wheelbase measuring λ in length. Angle ϕ_i denotes the orientation of the wheelchair robots relative to the Z_1 axis within the Z_1Z_2 cartesian plane. The centre of the given wheelchair is (x_i, y_i), and the angular velocity of the back left, and right wheels are given as V_{i_L} and V_{i_R}, respectively, at any given time t. The distance from the centre of the line

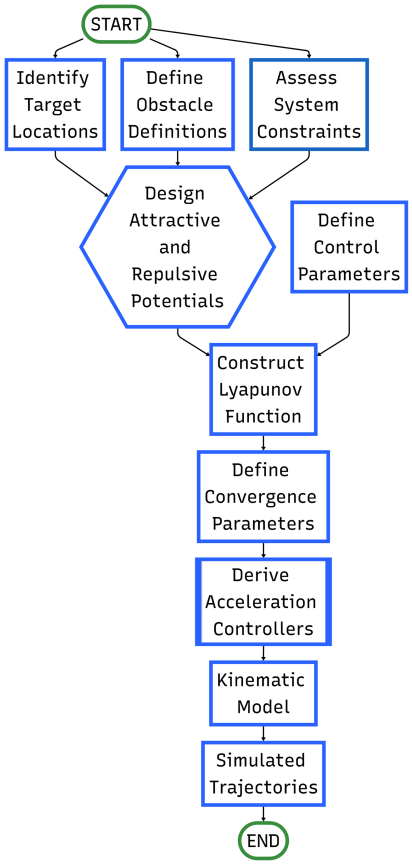

Fig. 2. Flowchart of the potential fields-based motion planning algorithm: From target identification to trajectory simulation.

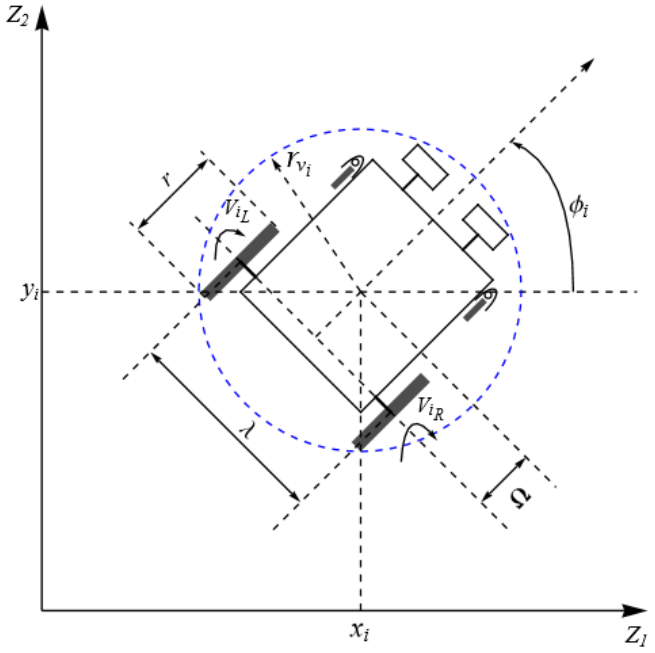

Fig. 3. A model of the ith wheelchair driven by two rear wheels and two front swivel wheels. Adopted and modified from Kumar *et al.* [20].

connecting the two driving wheels to the centre of mass of the wheelchair is Ω.

The wheelchairs are enclosed by the smallest possible imaginary circle, which acts as a protective shield during navigation around multiple stationary obstacles. As shown in Fig. 3, the protective circular shield has a radius defined as

$$r_{v_i} = \sqrt{\left(\frac{\lambda}{2}\right)^2 + \left(\Omega + \frac{r}{2}\right)^2} \tag{1}$$

and thus the configuration vector for the ith wheelchair robot is

$$\mathbf{x}_i = (x_i, y_i, \phi_i, V_{i_L}, V_{i_R}) \in \mathbb{R}^5.$$

It has been postulated that the wheelchairs can manoeuvre smoothly without any side slippage on the two back wheels and are undergoing pure rolling. Thus, with respect to their centres (x_i, y_i), the ensuing constraints are attained as

$$\dot{y}_i \cos\phi_i - \dot{x}_i \sin\phi_i - \dot{\phi}_i \Omega = 0, \tag{2}$$

$$\dot{x}_i \cos\phi_i + \dot{y}_i \sin\phi_i + \frac{\lambda}{2}\dot{\phi}_i - \frac{r}{2}\dot{V}_{i_R} = 0, \tag{3}$$

$$\dot{x}_i \cos\phi_i + \dot{y}_i \sin\phi_i - \frac{\lambda}{2}\dot{\phi}_i - \frac{r}{2}\dot{V}_{i_L} = 0. \tag{4}$$

The above constraints are in agreement with derivations attained by Solea *et al.* and Dhaouadi and Hatab [20]. When using LbCS, these constraints are addressed by embedding them in the kinematic model, designing an appropriate Lyapunov function in a reduced coordinate space to ensure target convergence, and using time-varying technique to bypass Brockett's condition. However, in practice, these constraints limit instantaneous maneuverability, increase convergence times, reduce workspace accessibility, and make the system more sensitive to disturbances. These restrictions for non-slippage of the wheelchair robots are required for proper integration into its kinematic model. Therefore, the kinematic model of the wheelchairs relative to their specified centres (x_i, y_i) can be derived by applying standard rigid body velocity transformations to the basic differential drive equations [46]. The resulting model is a modification of the kinematic equations presented by Kumar *et al.* for a single planar wheelchair robot [20] and is given by the following system of ODEs:

$$\left.\begin{aligned}
\dot{x}_i &= \frac{r}{2}\cos\phi_i(V_{i_R} + V_{i_L}) + \frac{r\Omega}{\lambda}\sin\phi_i(V_{i_L} - V_{i_R}) \\
\dot{y}_i &= \frac{r}{2}\sin\phi_i(V_{i_R} + V_{i_L}) + \frac{r\Omega}{\lambda}\cos\phi_i(V_{i_R} - V_{i_L}) \\
\dot{\phi}_i &= \frac{r}{2\lambda}(V_{i_R} - V_{i_L}) \\
\dot{V}_{i_R} &= u_{1_i} \\
\dot{V}_{i_L} &= u_{2_i}
\end{aligned}\right\}, \tag{5}$$

where u_{1_i} and u_{2_i} are the rotational accelerations of the wheelchair's left and right back wheels, respectively.

In a two-dimensional (2D) space, the location of wheelchair robots can be characterised by their linear components. Defining the position of the wheelchairs at time $t \geq 0$ as $x_i = (x_i(t), y_i(t))$ and direction angles given as $\phi_i = \phi_i(t)$, whereby the starting conditions are defined as $(x_i(t_0), y_i(t_0)) =: (x_{i_0}, y_{i_0})$, $\phi_i(t_0) = \phi_{i_0}$, $V_{i_R}(0) = V_{i_{R_0}}$ and $V_{i_L}(0) = V_{i_{L_0}}$.

The initial condition of the proposed multi-wheelchair system where $i \in \{1, 2, \dots, n\}$ upon suppressing t is given as

$$x_0 := \begin{bmatrix} x_{1_0} & y_{1_0} & \phi_{1_0} & V_{1_{L_0}} & V_{1_{R_0}} \\ x_{2_0} & y_{2_0} & \phi_{2_0} & V_{2_{L_0}} & V_{2_{R_0}} \\ \vdots & \vdots & \vdots & \vdots & \vdots \\ x_{n_0} & y_{n_0} & \phi_{n_0} & V_{n_{L_0}} & V_{n_{R_0}} \end{bmatrix}^T \in \mathbb{R}^{5n}.$$

Subsequently, the state vector of the system is given as

$$\mathbf{x} := \begin{bmatrix} x_1 & y_1 & \phi_1 & V_{1_L} & V_{1_R} \\ x_2 & y_2 & \phi_2 & V_{2_L} & V_{2_R} \\ \vdots & \vdots & \vdots & \vdots & \vdots \\ x_n & y_n & \phi_n & V_{n_L} & V_{n_R} \end{bmatrix}^T \in \mathbb{R}^{5n}.$$

5. Problem Formulation

Consider $n \in \mathbb{N}$ wheelchairs in a workspace cluttered with stationary $g \in \mathbb{N}$ disk, $m \in \mathbb{N}$ elliptic and $q \in \mathbb{N}$ line segment obstacles. The ultimate goal for each wheelchair is to navigate from their initial configuration, avoid obstacles and collisions, adhere to system restrictions and limitations and converge to a designated target.

Definition 5.1. The multi-wheelchair systems' equilibrium state is

$$\mathbf{x}_e := (\mathbf{x}_{1_e}, \mathbf{x}_{2_e}, \dots, \mathbf{x}_{n_e}) \in \mathbb{R}^{5n}, \tag{6}$$

where

$$\mathbf{x}_{i_e} := (\tau_{1_i}, \tau_{2_i}, \phi_{i_f}, 0, 0) \in \mathbb{R}^5,$$

where $i \in \{1, 2, \dots, n\}$ and ϕ_{i_f} is the final orientation of the i*th* wheelchair as it reaches its designated target.

Definition 5.2. The target for the i*th* wheelchair robot is a disk with centre (τ_{1_i}, τ_{2_i}). It is described as the set

$$T_i := \{(Z_1, Z_2) \in \mathbb{R}^2 : (Z_1 - \tau_{1_i})^2 + (Z_2 - \tau_{2_i})^2 \leq r_{\tau_i}^2\}.$$

Definition 5.3. The j*th* stationary solid obstacle is a disk with centre (w_{1_j}, w_{2_j}) and radius r_{W_j}. It is described as the set

$$W_j := \{(Z_1, Z_2) \in \mathbb{R}^2 : (Z_1 - w_{1_j})^2 + (Z_2 - w_{2_j})^2 \leq r_{W_j}^2\}.$$

Definition 5.4. The kth stationary solid obstacle is an ellipse centred at (f_{1_k}, f_{2_k}) with width $a_k > 0$ and height $b_k > 0$. It is described as the set

$$F_k := \left\{(Z_1, Z_2) \in \mathbb{R}^2 : \left(\frac{Z_1 - f_{1_k}}{a_k}\right)^2 + \left(\frac{Z_2 - f_{2_k}}{b_k}\right)^2 \leq 1\right\}.$$

Definition 5.5. The pth stationary obstacle is a line segment from the point (c_{1_p}, d_{1_p}) to the point (c_{2_p}, d_{2_p}). It is described as the set

$$Q_p := \{(Z_1, Z_2) \in \mathbb{R}^2 : (Z_1 - c_{1_p} - \varphi(c_{2_p} - c_{1_p}))^2 + (Z_2 - d_{1_p} - \varphi(d_{2_p} - d_{1_p}))^2 = 0\},$$

where $\varphi_p \in [0, 1]$.

6. Design of Acceleration-based Controllers

6.1. *Target attraction and obstacle avoidance functions*

The following attractive and repulsive functions have been designed to be part of the total potential.

6.1.1. *Target attraction function*

The attraction function that will ensure that the i*th* wheelchair robot will converge successfully toward its designated target is

$$T_i = \frac{1}{2}((x_i - \tau_{1_i})^2 + (y_i - \tau_{2_i})^2 + V_{i_R}^2 + V_{i_L}^2). \tag{7}$$

6.1.2. *Stationary obstacles avoidance functions*

This paper will simulate real-world cases whereby one scenario would be a children's outdoor park where there will be play areas/stations simulated as disks, ellipses or lines and the other would be an office workspace designed using line segments and stationary objects such as office chairs cluttered in the space represented as disks or ellipses.

- *Disk Obstacle Avoidance Function*
  For the i*th* wheelchair robot to avoid the j*th* disk obstacle, the following function is designed:
  $$W_{i_j} = \frac{1}{2}((x_i - w_{1_j})^2 + (y_i - w_{2_j})^2 - (r_{W_j} + r_{v_i})^2) \tag{8}$$
  for $i \in \{1, 2, \dots, n\}$ and $j \in \{1, 2, \dots, g\}$.
- *Elliptic Obstacle Avoidance Function*
  For the i*th* wheelchair robot to avoid the kth elliptical obstacle, the following avoidance function is constructed:
  $$F_{i_k} = \frac{1}{2}\left(\left(\frac{x_i - f_{1_k}}{a_k + r_{v_i}}\right)^2 + \left(\frac{y_i - f_{2_k}}{b_k + r_{v_i}}\right)^2 - 1\right) \tag{9}$$
  for $i \in \{1, 2, \dots, n\}$ and $k \in \{1, 2, \dots, m\}$.

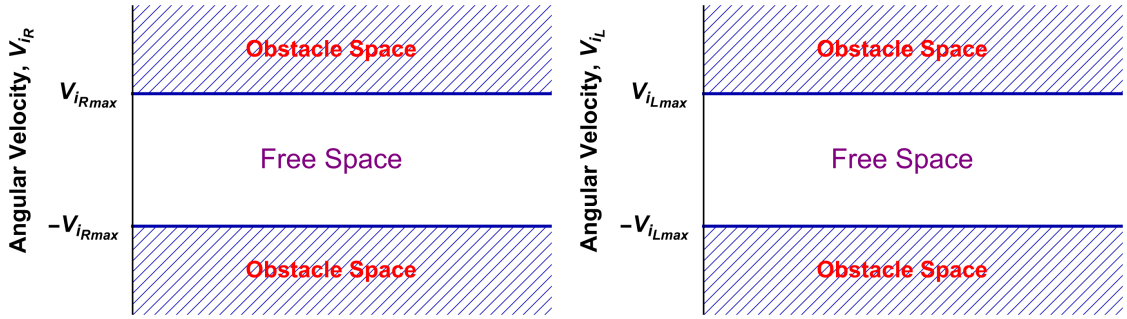

(a) (b)

Fig. 4. The restriction on the angular velocities $V_{i_{R_{\max}}}$ and $V_{i_{L_{\max}}}$ are constrained by obstacles space. (a) Restrictions on V_{i_R} and (b) Restrictions on V_{i_L}.

- *Line Segment Obstacle Avoidance*
  In this paper, the line segments are used to construct rectangular obstacles representing playhouses and triangular obstacles representing a play area; line segments are used to construct the walls in the design of an office space with cubicles. Considering there are pth line segments from the points (c_{1_p}, d_{1_p}) to (c_{2_p}, d_{2_p}) for $p \in \{1, 2, \dots, q\}$, the following function is designed as

$$Q_{i_p} = \frac{1}{2}((x_i - X_{i_p})^2 + (y_i - Y_{i_p})^2 - r_i^2) \tag{10}$$

for the ith wheelchair robot to avoid the pth line segment obstacle using the Minimum Distance Technique (MDT), where $X_{i_p} = c_{1_p} + \varphi_{i_p}(c_{2_p} - c_{1_p})$ and $Y_{i_p} = d_{1_p} + \varphi_{i_p}(d_{2_p} - d_{1_p})$, such that

$$\varphi_{i_p} = \begin{cases} 0 & \text{if } \varrho_{i_p} \le 0, \\ \varrho_{i_p} & \text{if } 0 < \varrho_{i_p} < 1, \\ 1 & \text{if } \varrho_{i_p} \ge 1 \end{cases} \tag{11}$$

and

$$\varrho_{i_p} = \frac{(c_{2_p} - c_{1_p})(x_i - c_{1_p}) + (d_{2_p} - d_{1_p})(y_i - d_{1_p})}{((c_{2_p} - c_{1_p})^2 + (d_{2_p} - d_{1_p})^2} \tag{12}$$

for $p \in \{1, 2, \dots, q\}$. The point (X_{i_p}, Y_{i_p}) on the line segment is the closest point to ith wheelchair robot, and the ith wheelchair robot will avoid this point at any given time $t \ge 0$.

6.1.3. *Inter-agent collision avoidance function*

In this study, since multiple wheelchair robots will be navigating a common workspace, there is a need to ensure that they do not collide with each other as they avoid other stationary obstacles and converge towards their desired targets. The inter-agent collision avoidance function is designed as

$$H_{i_h} = \frac{1}{2}((x_i - x_h)^2 + (y_i - y_h)^2 - (r_i + r_h)^2) \tag{13}$$

for $i, h \in \{1, 2, \dots, n\}$ and $i \ne h$.

6.1.4. *Artificial obstacle avoidance function*

Since the wheelchair robots will be applied in real-world applications, the back wheels have restrictions in their angular velocities and can only be facilitated in the LbCS with the inclusion of artificial obstacles. Let $V_{i_{R_{\max}}}$ and $V_{i_{L_{\max}}}$ be the maximum velocity of the right and left back wheels of the ith wheelchair, respectively. Then, at any given time $t \ge 0$ $V_{i_R} \le V_{i_{R_{\max}}}$ and $V_{i_L} \le V_{i_{L_{\max}}}$.

In order for the wheelchair robots to navigate successfully within limitations, the following *artificial obstacle avoidance* functions are designed as

$$A_i = \frac{1}{2}(V_{i_{R_{\max}}}^2 - V_{i_R}^2) \tag{14}$$

and

$$B_i = \frac{1}{2}(V_{i_{L_{\max}}}^2 - V_{i_L}^2) \tag{15}$$

for $i \in \{1, 2, \dots, n\}$.

6.1.5. *Auxiliary functions for the wheelchair robots*

To guarantee that the nonlinear acceleration controllers of the ith wheelchair vanish at its target, an auxiliary function is considered as follows:

$$G_i = \frac{1}{2}((x_i - \tau_{1_i})^2 + (y_i - \tau_{2_i})^2). \tag{16}$$

6.2. *The total potential*

Consequently, combining Eqs. (7)–(13) and establishing *control parameters*, $\alpha_i > 0$ (target attraction), $\beta_{ik} > 0$ (elliptic

obstacle avoidance), $\gamma_{ij} > 0$ (disk obstacle avoidance), $\rho_{ip} > 0$ (line obstacle avoidance), $\epsilon_{ih} > 0$ (coupling), $\mu_i > 0$, and $\sigma_i > 0$ (artificial obstacle avoidance) where $h, i, j, k, p \in \mathbb{N}$ a Lyapunov function is obtained as

$$L(\mathbf{x}) = \sum_{i=1}^{n}\left(\alpha_i T_i + G_i\left(\sum_{k=1}^{m}\frac{\beta_{ik}}{F_{i_k}} + \sum_{j=1}^{g}\frac{\gamma_{ij}}{W_{i_j}} + \sum_{p=1}^{q}\frac{\rho_{ip}}{Q_{i_p}}\right)\right) + \sum_{i=1}^{n} G_i\left(\sum_{\substack{h=1\\ i\neq h}}^{n}\frac{\epsilon_{ih}}{H_{i_h}} + \frac{\mu_i}{A_i} + \frac{\sigma_i}{B_i}\right). \quad (17)$$

6.2.1. *Acceleration-based controllers*

The time derivative of (17) along the trajectory of system (5) is

$$\dot{L}(\mathbf{x}) = \sum_{i=1}^{n}\left(\frac{\partial L}{\partial x_i}\dot{x}_i + \frac{\partial L}{\partial y_i}\dot{y}_i + \frac{\partial L}{\partial \phi_i}\dot{\phi}_i + \alpha_i V_{i_R}\dot{V}_{i_R} + \alpha_i V_{i_L}\dot{V}_{i_L}\right) + \sum_{i=1}^{n}\left(\frac{\mu_i G_i}{A_i^2}V_{i_R}\dot{V}_{i_R} + \frac{\sigma_i G_i}{B_i^2}V_{i_L}\dot{V}_{i_L}\right). \quad (18)$$

By substituting the kinematic model given by system (5) into (18), it could be shown that

$$\begin{aligned}\dot{L}(\mathbf{x}) = &\sum_{i=1}^{n}\left(\frac{\partial L}{\partial x_i}\frac{r}{2}\cos\phi_i - \frac{\partial L}{\partial x_i}\frac{r\Omega}{\lambda}\sin\phi_i + \alpha_i u_{1_i}\right)V_{i_R}\\ &+ \sum_{i=1}^{n}\left(\frac{\partial L}{\partial y_i}\frac{r\Omega}{\lambda}\cos\phi_i + \frac{\partial L}{\partial y_i}\frac{r}{2}\sin\phi_i + \frac{\mu_i G_i}{A_i^2}u_{1_i}\right)V_{i_R}\\ &+ \sum_{i=1}^{n}\left(\frac{\partial L}{\partial x_i}\frac{r}{2}\cos\phi_i + \frac{\partial L}{\partial x_i}\frac{r\Omega}{\lambda}\sin\phi_i + \alpha_i u_{2,i}\right)V_{i_L}\\ &+ \sum_{i=1}^{n}\left(\frac{\partial L}{\partial y_i}\frac{r}{2}\sin\phi_i - \frac{\partial L}{\partial y_i}\frac{r\Omega}{\lambda}\cos\phi_i + \frac{\sigma_i G_i}{B_i^2}u_{2,i}\right)V_{i_L}.\end{aligned}$$

Defining $\xi_{1_i}, \xi_{2_i} > 0$ as *convergence parameters*, let

$$\begin{aligned}-\xi_{1_i}V_{i_R}^2 = &\frac{\partial L}{\partial x_i}\left(\frac{r}{2}\cos\phi_i - \frac{r\Omega}{\lambda}\sin\phi_i\right)V_{i_R}\\ &+ \left(\frac{\partial L}{\partial y_i}\left(\frac{r}{2}\sin\phi_i + \frac{r\Omega}{\lambda}\cos\phi_i\right)\right.\\ &\left.+ \alpha_i u_{1,i} + \frac{\mu_i G_i}{A_i^2}u_{1_i}\right)V_{i_R}\end{aligned} \quad (19)$$

and

$$\begin{aligned}-\xi_{2_i}V_{i_L}^2 = &\frac{\partial L}{\partial x_i}\left(\frac{r}{2}\cos\phi_i + \frac{r\Omega}{\lambda}\sin\phi_i\right)V_{i_L}\\ &+ \left(\frac{\partial L}{\partial y_i}\left(\frac{r}{2}\sin\phi_i - \frac{r\Omega}{\lambda}\cos\phi_i\right)\right.\\ &\left.+ \alpha_i u_{2,i} + \frac{\sigma_i G_i}{B_i^2}u_{2_i}\right)V_{i_L}.\end{aligned} \quad (20)$$

Consequently, the following functions define the *acceleration-based controllers* of the multiple wheelchair robots:

$$\left.\begin{aligned}u_{1_i} = &\frac{-A_i^2}{\mu_i G_i + \alpha_i A_i^2}\left(\frac{\partial L}{\partial x_i}r\left(\frac{\cos\phi_i}{2} - \frac{\Omega}{\lambda}\sin\phi_i\right) + \xi_{1,i}V_{i_R}\right)\\ &- \frac{A_i^2}{\mu_i G_i + \alpha_i A_i^2}\frac{\partial L}{\partial y_i}r\left(\frac{1}{2}\sin\phi_i + \frac{\Omega}{\lambda}\cos\phi_i\right)\\ u_{2_i} = &\frac{-B_i^2}{\sigma_i G_i + \alpha_i B_i^2}\left(\frac{\partial L}{\partial x_i}r\left(\frac{\cos\phi_i}{2} + \frac{\Omega}{\lambda}\sin\phi_i\right) + \xi_{1,i}V_{i_L}\right)\\ &- \frac{B_i^2}{\sigma_i G_i + \alpha_i B_i^2}\frac{\partial L}{\partial y_i}r\left(\frac{1}{2}\sin\phi_i - \frac{\Omega}{\lambda}\cos\phi_i\right)\end{aligned}\right\}. \quad (21)$$

6.3. *Stability analysis*

Theorem 6.1. *The equilibrium point* $\mathbf{x}_e$ *of system* (5) *is stable if the acceleration controllers* u_{1_i} *and* u_{2_i} *for* $i \in \{1, 2, \ldots, n\}$ *are defined as in Eq.* (21).

Proof.

(1) $L(\mathbf{x}) > 0, \forall\, \mathbf{x} \in D(L(\mathbf{x})), \mathbf{x} \neq \mathbf{x}_e$ over the domain:

$$\begin{aligned}D(L(\mathbf{x})) := \{\mathbf{x} \in \mathbb{R}^{5n} \mid &F_{i_k}(\mathbf{x}) > 0, W_{i_j}(\mathbf{x}) > 0,\\ &Q_{i_p}(\mathbf{x}) > 0, H_{i_h}(\mathbf{x}) > 0, A_i(\mathbf{x}) > 0,\\ &B_i(\mathbf{x}) > 0, \forall\, h, i, j, k, p \in \mathbb{N}\}\end{aligned}$$

where $i, h \in \{1, \ldots, n\}$ with $i \neq h$, $j \in \{1, \ldots, g\}$, $p \in \{1, \ldots, q\}$ and $k \in \{1, \ldots, m\}$.

(2) $L(\mathbf{x}_e) = 0$.

(3) By using (19) and (20), it could be be easily shown that

$$\dot{L}(\mathbf{x}) = -\sum_{i=1}^{n}(\xi_{1_i}V_{i_R}^2 + \xi_{2_i}V_{i_L}^2) \leq 0$$

for all $\mathbf{x} \in D(L(\mathbf{x}))$.

Thus, the equilibrium point $\mathbf{x}_e$ of system (5) is stable. □

7. Simulations Results

Simulation results for two cases of multiple wheelchair-like robots navigating within a disordered environment filled with stationary obstacles are presented in this section. System (5) was numerically simulated using the RK4 method (Runge–Kutta Method) in Wolfram Mathematica 13.3 software. To achieve the desired results, a number of sequential Mathematica commands were executed. Before the commands are executed specific initial conditions (positions and orientations) of the wheelchair robots and obstacles were generated. Also, the convergence, collision and obstacle avoidance parameters have to be determined through brute-force technique. For some initial conditions fine-tuning the parameters becomes necessary to identify combinations that effectively demonstrated the controllers' ability to achieve the primary objectives, namely, successful navigation to designated targets while ensuring obstacle avoidance, collision avoidance between wheelchairs, and adherence to system constraints within these representative scenarios. The aim of this parameter and initial condition selection was primarily focused on illustrating the controller's capabilities and validating the proof-of-concept.

The simulation examples are performed within a numerical environment where quantities such as distance and time are represented by dimensionless values known as Simulation Units (SU). This approach provides a scalable framework, allowing the results to be adapted to various physical contexts. For instance, a velocity within the simulation represents the movement of spatial SU per temporal SU. To contextualize these findings for a real-world system, a characteristic length (e.g. meters) and time (e.g. seconds) can be defined to convert the dimensionless simulation outputs into meaningful physical units (e.g. m/s).

Example 7.1. This scenario demonstrates the efficiency of the designed acceleration-based controllers using multiple wheelchair robots in a simulated park environment. Figure 5 shows the initial setup, including the starting positions of the three wheelchair robots, their respective targets, and the stationary obstacles (Playhouse 1, Playhouse 2, Water Fountain, and Hopscotch Field) as labelled.

Figure 6 illustrates the resulting trajectories of the multiple wheelchair robots navigating the constrained environment. Within this figure, specific labels identify each robot and its corresponding start and end points. The abbreviation "WC i" refers to Wheelchair i, where $i \in \{1, 2, 3\}$ denotes the index of the individual robot. Consequently, "IP WC i" marks the Initial Position from which Wheelchair i begins its navigation, and "Target WC i" indicates the designated target location for Wheelchair i.

All necessary setup details, such as initial coordinates, wheelchair dimensions, and control parameters,

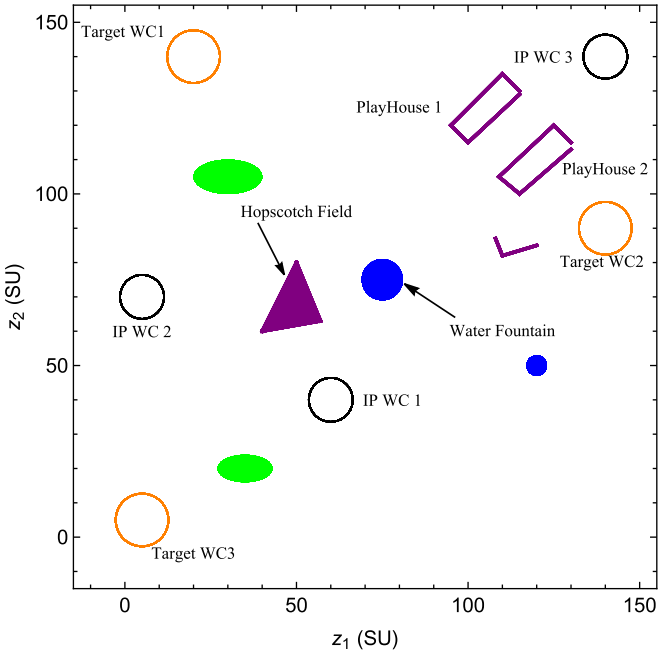

Fig. 5. Initial positions of three wheelchair robots in a virtual children's play park.

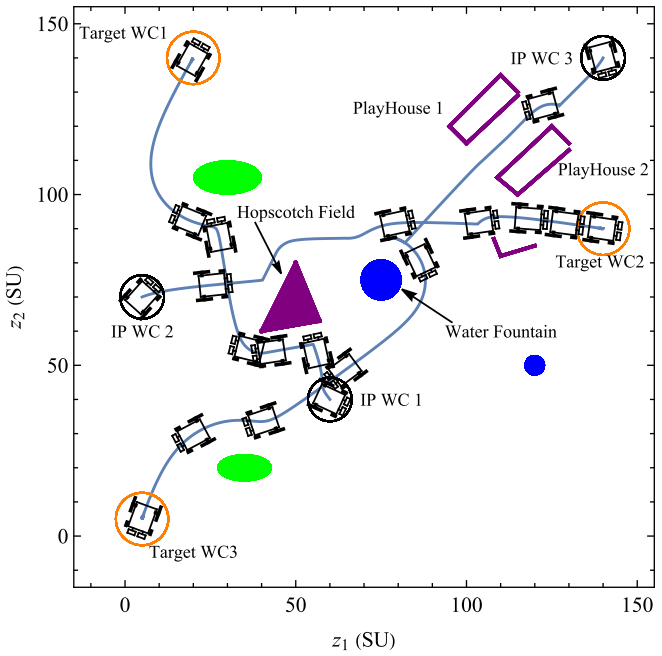

Fig. 6. Trajectory of the multiple wheelchair robots.

along with restrictions and limitations derived from the robot dynamics, are provided in Table 1. The objective requires the wheelchair robots to navigate from their initial positions to their target locations while avoiding stationary obstacles and inter-robot collisions. This scenario

Table 1. Numerical values of initial states, constraints, and control parameters for the wheelchair robots.

Initial Conditions	
Positions	$(x_{1_0}, y_{1_0}) = (60, 40)$, $(x_{2_0}, y_{2_0}) = (5, 70)$, $(x_{3_0}, y_{3_0}) = (140, 140)$
Orientations	ϕ_{i_0} was randomized within $[-2\pi, 2\pi]$ for $i \in \{1, 2, 3\}$.
System constraints and setup	
Targets	$(\tau_{1_1}, \tau_{2_1}) = (20, 140)$, $(\tau_{1_2}, \tau_{2_2}) = (140, 90)$, $(\tau_{1_3}, \tau_{2_3}) = (5, 5)$
Wheelchair dimensions	$r = 2, \lambda = 4, \Omega = 3$
Max wheel velocity	1 rad/SU
Disk obstacles	$(w_{1_1}, w_{2_1}) = (75, 75), r_{W_1} = 6$ $(w_{1_2}, w_{2_2}) = (120, 50), r_{W_2} = 3$
Elliptic obstacles	$(f_{1_1}, f_{2_1}) = (30, 105)$, $a_1 = 10, b_1 = 5$ $(f_{1_2}, f_{2_2}) = (35, 20)$, $a_2 = 8, b_2 = 4$
Line obstacles	
$(c_{1_1}, d_{1_1}) = (40, 60)$	$(c_{2_1}, d_{2_1}) = (50, 80)$
$(c_{1_2}, d_{1_2}) = (50, 80)$	$(c_{2_2}, d_{2_2}) = (57, 63)$
$(c_{1_3}, d_{1_3}) = (40, 60)$	$(c_{2_3}, d_{2_3}) = (57, 63)$
$(c_{1_4}, d_{1_4}) = (110, 82)$	$(c_{2_4}, d_{2_4}) = (120, 85)$
$(c_{1_5}, d_{1_5}) = (110, 82)$	$(c_{2_5}, d_{2_5}) = (108, 87)$
$(c_{1_6}, d_{1_6}) = (100, 115)$	$(c_{2_6}, d_{2_6}) = (115, 129)$
$(c_{1_7}, d_{1_7}) = (109, 105)$	$(c_{2_7}, d_{2_7}) = (125, 120)$
$(c_{1_8}, d_{1_8}) = (100, 115)$	$(c_{2_8}, d_{2_8}) = (95, 120)$
$(c_{1_9}, d_{1_9}) = (110, 135)$	$(c_{2_9}, d_{2_9}) = (95, 120)$
$(c_{1_{10}}, d_{1_{10}}) = (115, 100)$	$(c_{2_{10}}, d_{2_{10}}) = (109, 105)$
$(c_{1_{11}}, d_{1_{11}}) = (115, 100)$	$(c_{2_{11}}, d_{2_{11}}) = (130, 113)$
$(c_{1_{12}}, d_{1_{12}}) = (115, 130)$	$(c_{2_{12}}, d_{2_{12}}) = (110, 135)$
$(c_{1_{13}}, d_{1_{13}}) = (130, 115)$	$(c_{2_{13}}, d_{2_{13}}) = (125, 120)$
Control parameters	
Target convergence	$\alpha_i = 1$ for $i \in \{1, 2, 3\}$
Disk obstacle avoidance	$\gamma_{ij} = 0.05$ for $i \in \{1, 2, 3\}$ and $j \in \{1, 2\}$
Elliptic obstacle avoidance	$\beta_{ik} = 0.05$ for $i \in \{1, 2, 3\}$ and $k \in \{1, 2\}$
Line obstacle avoidance	$\rho_{ip} = 0.001$ for $i \in \{1, 2, 3\}$
avoidance	and $p \in \{1, 2, \ldots, 13\}$
Coupling	$\epsilon_{ih} = 0.001$ for $i, h \in \{1, 2, 3\}$ and $i \neq h$
Artificial obstacle avoidance	$\mu_i = \sigma_i = 0.001$ for $i \in \{1, 2, 3\}$
Convergence	$\xi_{1i} = \xi_{2i} = 500$ for $i \in \{1, 2, 3\}$

highlights specific behaviours: for example, Wheelchair 3 (WC3) successfully navigates the narrow space between the two "Playhouse" obstacles, demonstrating line obstacle avoidance. Furthermore, the robots exhibit effective turning capabilities at corners, such as avoiding the triangular "opscotch Field" obstacle, demonstrating differential steering. The Lyapunov function value and its time derivative are shown in Figs. 7(a) and 7(b), respectively. These plots illustrate the decrease in the Lyapunov function value as the wheelchairs converge toward their designated targets. Figures 8(a) and 8(b) show the angular velocities of the right and left wheels for all wheelchair robots, respectively. Positive angular velocities generally correspond to forward acceleration or motion, while negative values indicate deceleration or reverse motion components during maneuvering.

Example 7.2. This scenario has a virtual setup of an office environment containing cubicles and walkways. Figure 9 shows the initial and target location for the four wheelchair robots, their targets and the location of the obstacles. There are four pathways shown, and a wheelchair robot is situated in each of the pathways, destined to the opposite side of the pathways. The wheelchair robots are to avoid stationary obstacles (disks, ellipses, corners and edges of the cubicles) and collisions with other moving wheelchair robots. Table 2 provides conditions, constraints and control parameters if they differ from Example 7.1. Figure 10 shows the trajectories of all four wheelchair robots from their initial configuration space to their final destination. The wheelchair robots approach the disk obstacle situated at the intersection of the pathways, avoiding collisions and obstacles and reaching their targets safely. The total potential and its time derivative are similar to case one. Figures 11(a) and 11(b) show the angular velocities of the right and left wheels of all the wheelchair robots, respectively.

8. Discussion

The initiation and use of robotic wheelchairs is enhancing the lives of PSN in challenging environments that were traditionally deemed impossible. Conventionally, complications for wheelchairs is the requirement for human support or command to assist in moving the wheelchair. However, some cases where the PSNs are severely disabled and do not have the ability to provide such aid or commands to move the wheelchair will be disadvantaged.

In this paper, as an application of the LbCS methodology, a set of acceleration-based controllers were derived to maneuver multiple wheelchairs in a cluttered environment. Conventional wheelchair systems typically require continuous human support or explicit commands to initiate and sustain motion [12–14, 19, 21]. This limits usability for persons with severe disabilities. In contrast, the approach based on the LbCS methodology proposed removes the dependence on human input, enabling fully autonomous navigation in cluttered environments. Unlike traditional velocity-based controllers (example, Kumar *et al.* [20]), the acceleration-based control laws generate smoother transitions in velocity, thereby reducing sharp changes that cause

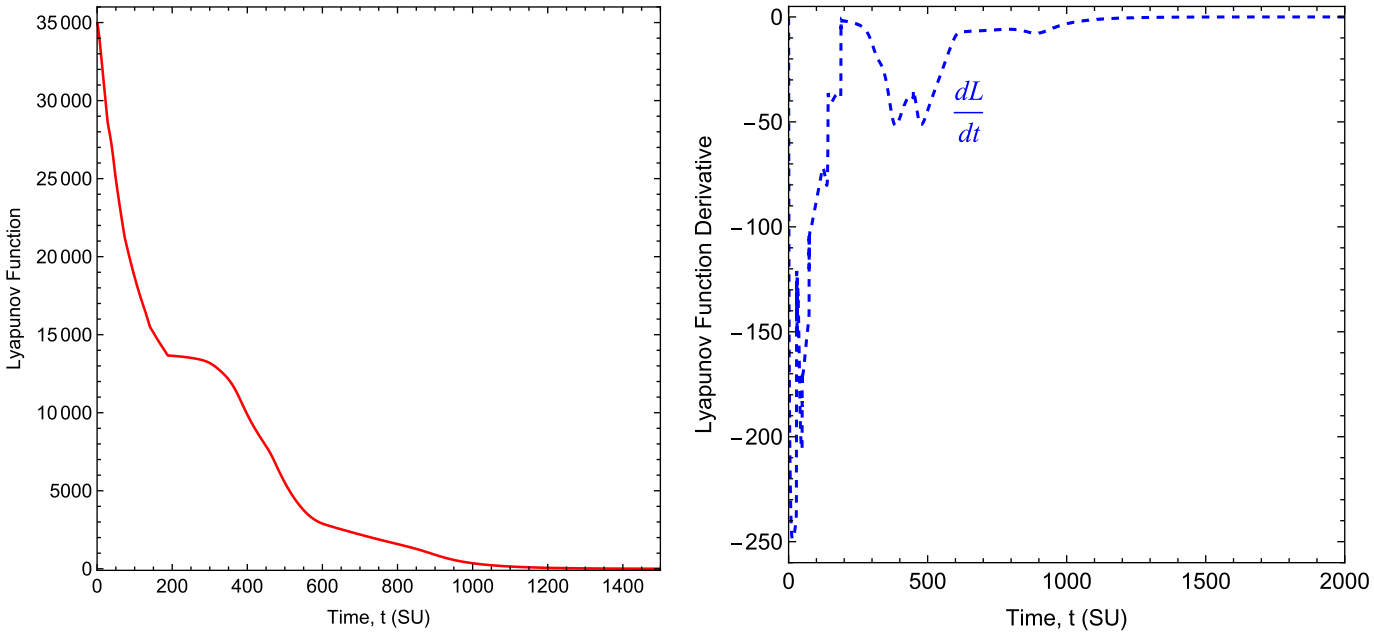

(a) (b)

Fig. 7. Lyapunov function and its time derivative. (a) Decreasing total potential and (b) Total potential derivative.

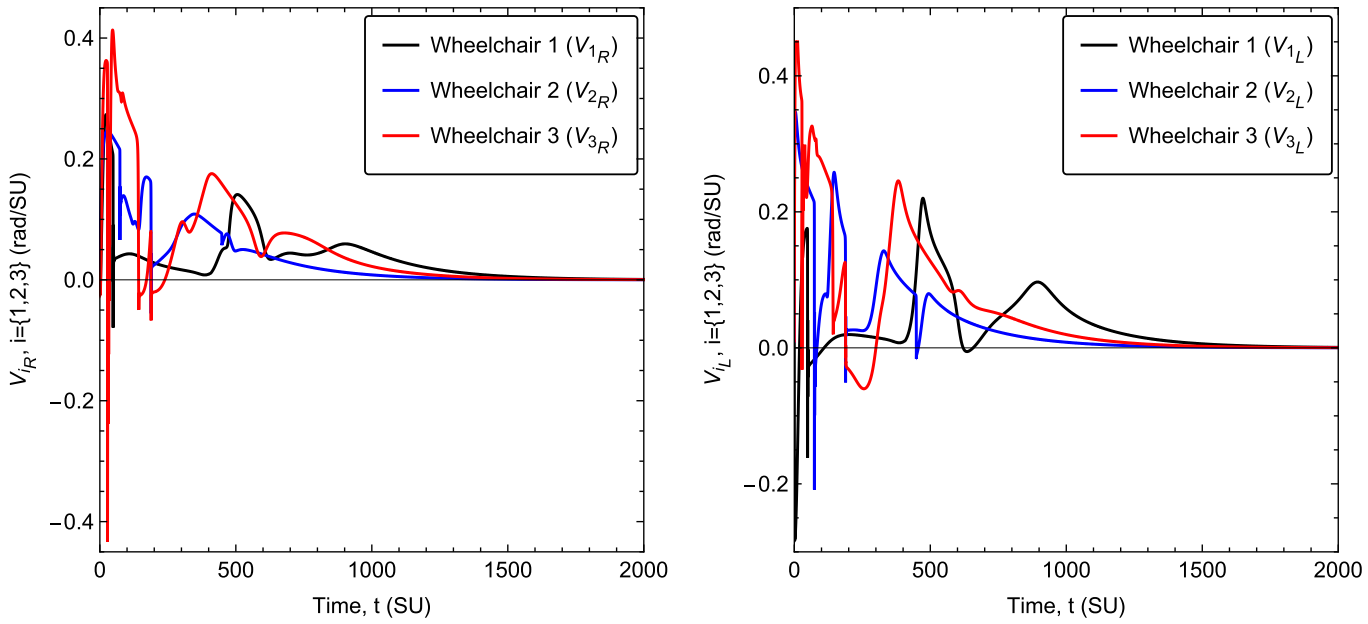

(a) (b)

Fig. 8. Angular velocities of wheelchair robots. (a) Angular velocities of the right rear wheel (V_{i_R}) for the three wheelchair robots and (b) Angular velocities of the left rear wheel (V_{i_L}) for the three wheelchair robots.

discomfort to users and lead to faster wear of mechanical components. This feature improves both user comfort and system longevity. By construction, the LbCS framework provides formal Lyapunov stability guarantees, ensuring that the wheelchair trajectories remain collision-free and converge safely. This theoretical guarantee is not present in several prior systems (examples, Grewal *et al.* [47], Foresi *et al.* [48], and Jayacody *et al.* [49]), which depend on reactive

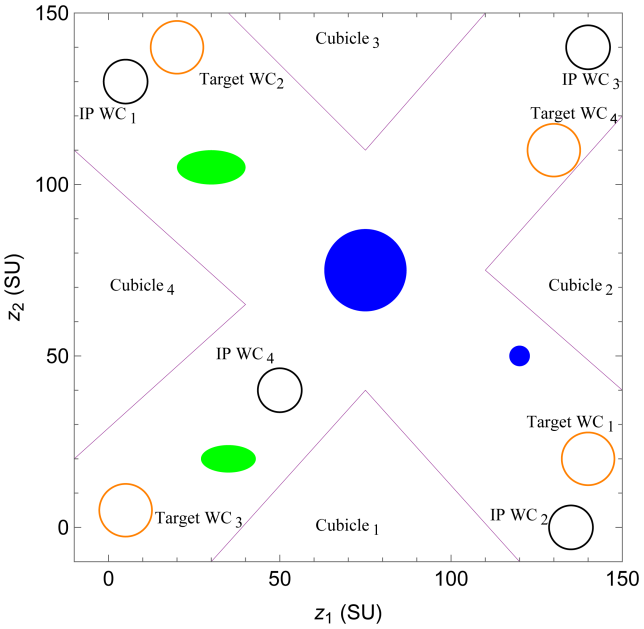

Fig. 9. A virtual office workshop navigation with four wheelchair robots.

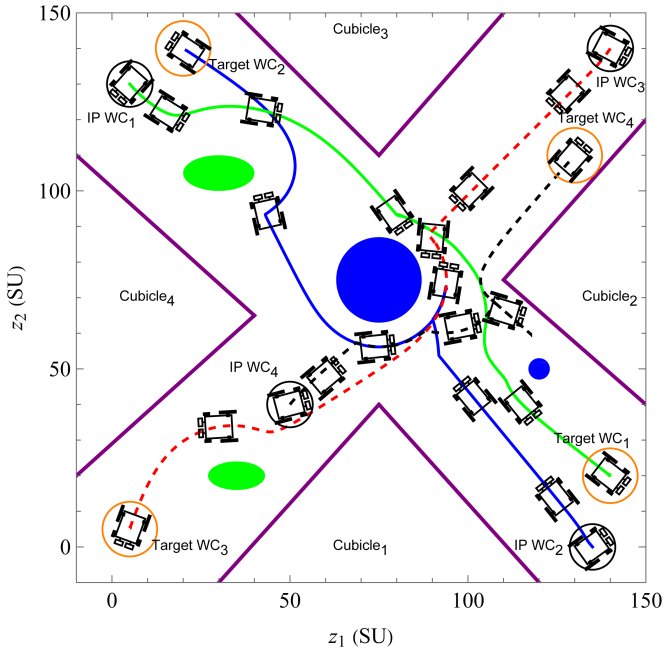

Fig. 10. Trajectories of the multiple wheelchair robots.

Table 2. Numerical values of parameters and initial states differing from Examples 7.1 for 7.2.

Initial conditions	
Positions	$(x_{1_0}, y_{1_0}) = (135, 0)$, $(x_{2_0}, y_{2_0}) = (5, 130)$, $(x_{3_0}, y_{3_0}) = (140, 140)$, $(x_{4_0}, y_{4_0}) = (50, 40)$
System constraints and setup	
Targets	$(\tau_{1_1}, \tau_{2_1}) = (20, 140)$, $(\tau_{1_2}, \tau_{2_2}) = (140, 20)$, $(\tau_{1_3}, \tau_{2_3}) = (5, 5)$, $(\tau_{1_4}, \tau_{2_4}) = (130, 110)$
Disk obstacles	$r_{W_1} = 12$
Line obstacles	
$(c_{1_1}, d_{1_1}) = (35, 150)$	$(c_{2_1}, d_{2_1}) = (75, 110)$
$(c_{1_2}, d_{1_2}) = (75, 110)$	$(c_{2_2}, d_{2_2}) = (110, 150)$
$(c_{1_3}, d_{1_3}) = (150, 120)$	$(c_{2_3}, d_{2_3}) = (110, 75)$
$(c_{1_4}, d_{1_4}) = (110, 75)$	$(c_{2_4}, d_{2_4}) = (150, 40)$
$(c_{1_5}, d_{1_5}) = (30, -10)$	$(c_{2_5}, d_{2_5}) = (75, 40)$
$(c_{1_6}, d_{1_6}) = (75, 40)$	$(c_{2_6}, d_{2_6}) = (120, -10)$
$(c_{1_7}, d_{1_7}) = (-10, 20)$	$(c_{2_7}, d_{2_7}) = (40, 65)$
$(c_{1_8}, d_{1_8}) = (-10, 110)$	$(c_{2_8}, d_{2_8}) = (40, 65)$
Control parameters	
Artificial obstacle avoidance	$\mu_i = \sigma_i = 0.01$ for $i \in \{1, 2, 3, 4\}$

inputs and can be unstable in highly constrained environments. Moreover, the framework presented allows for pre-programmed, centrally coordinated multi-wheelchair navigation (as demonstrated in the children's park and office workspace simulations). This ensures collision-free, synchronized arrivals at target locations, which conventional systems relying on manual control cannot achieve.

8.1. *LbCS limitations*

Despite the advantages of LbCS for autonomous control, some notable drawbacks are as follows:

- The potential for the system to encounter local minima. Achieving optimal performance often requires careful parameter tuning, which can be tedious. Suboptimal parameter choices or challenging initial conditions may lead to non-optimal trajectories or exacerbate the local minima problem.
- Environment complexity gives rise to local minima issues, conservative trajectories, and difficulties in designing an appropriate Lyapunov function.
- Scalability issues arise due to the computational complexities in handling a large number of wheelchair robots or obstacles.

Future extensions may incorporate strategies such as randomized perturbations to escape spurious equilibria, navigation functions (e.g. Rimon–Koditschek potentials) that are provably free of local minima under certain conditions, or hybrid schemes combining LbCS with global planners or heuristic algorithms to ensure global completeness. These approaches would further strengthen the robustness of the proposed framework in highly cluttered environments. The advantages of using LbCS lie in its simplicity

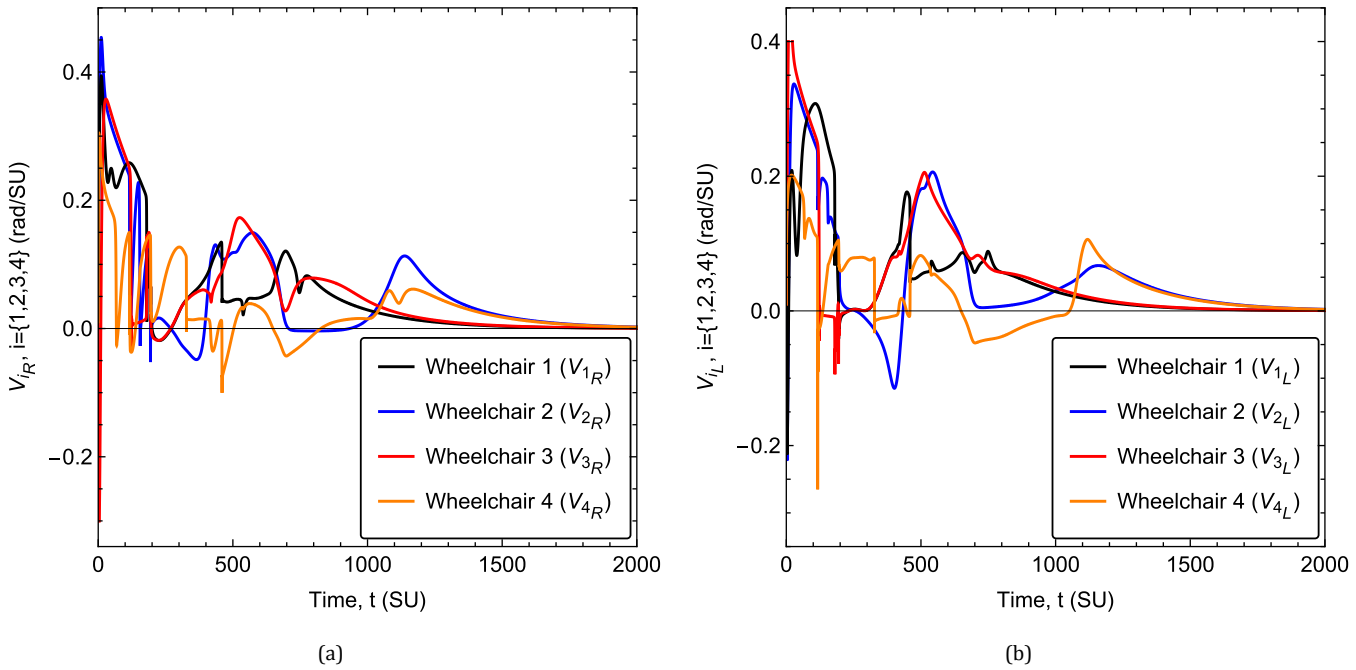

Fig. 11. Angular Velocities of wheelchair robots. (a) Angular velocities of the right rear wheel (V_{i_R}) for the four wheelchair robots and (b) Angular velocities of the right rear wheel (V_{i_R}) for the four wheelchair robots.

in designing continuous nonlinear controllers and its ability to incorporate mechanical constraints easily, compared to other motion control schemes in the literature. Although this approach includes distributed optimization, it does not ensure scalability. Increasing the number of wheelchair robots or obstacles increases environmental complexity and demands greater computing power and sensing capabilities to increase real-time responsiveness. However, these challenges can be significantly reduced with the rapid growth in processing power, memory capacity and storage, alongside decreasing hardware costs and the widespread use of GPS to reduce sensing limitations. In future, the development of quantum computers may eliminate scalability issues.

8.2. *Prototype implementation challenges*

It is important to reiterate that the findings presented in this paper are based on theoretical analysis and numerical simulations. While these simulations demonstrate the potential effectiveness of the proposed acceleration-based controllers under idealized conditions, experimental validation using physical wheelchair prototypes was not performed. Transitioning from simulation to real-world implementation introduces significant challenges that are not captured in the current model.

Real-world environments present complexities and uncertainties far exceeding those typically modelled in simulation. Factors such as uneven terrain, varying surface friction, unanticipated obstacles, sensor noise (e.g. from encoders, IMUs, or external perception systems), and real-time computational constraints can significantly impact controller performance and stability.

Furthermore, the kinematic model (5) assumes pure rolling and neglects wheel slippage. In practice, slippage is likely to occur, particularly on different surfaces, during rapid acceleration/deceleration, or turning maneuvers. This discrepancy between the ideal model and physical reality can lead to inaccuracies in state estimation and degraded tracking performance. Other unmodeled dynamics, including actuator limitations (torque saturation, response delays), friction in joints and transmissions, and component tolerances, would also need to be addressed in a physical implementation.

Addressing these challenges requires robust state estimation techniques, adaptive control strategies capable of handling model mismatch and disturbances, careful sensor calibration, statistical reliability studies through multiple-run simulations and hardware-in-the-loop testing before deployment. Physical real-world environmental interactions and management require robot operating system (ROS) for integrating sensor suites (for instance, the use light detection and ranging (LiDAR), cameras, and simulatneous localization and mapping(SLAM)). Therefore, while the simulation results provide valuable insights and a proof-of-concept, experimental validation on physical wheelchair robots is essential future work to fully assess the practical applicability and robustness of the proposed LbCS-based acceleration controllers in realistic assistive technology scenarios.

9. Conclusion

The study of wheelchair-mobile robot manoeuvres presents how the field of robotics can be helpful for people with special needs with the advancement of new technologies. This study presented a set of novel stabilizing nonlinear time-invariant continuous acceleration-based controllers for multiple wheelchair robots in constrained environments. The controllers were developed using the LbCS. These controllers successfully demonstrated robust obstacle avoidance and smooth navigation in complex, constrained environments through numerical simulations. The results highlight the ability of the controllers to ensure the wheelchairs reach their target positions with minimal human interaction, providing an efficient solution for assistive robotic systems. While LbCS presents advantages in autonomous mobility and collision avoidance, challenges like local minima and fine-tuning remain.

This work is an initial step in extending LbCS methodology to swarm navigation problems. A detailed benchmarking exercise, covering accuracy, efficiency, systematic robustness studies, incorporating error analysis and confidence intervals across multiple runs and experimental conditions, to complement the theoretical guarantees and computational cost relative to other established approaches, will form the basis of our future work, where LbCS can be evaluated within standardized multi-agent navigation benchmarks. Future work will also involve real-world testing with a prototype and further refinement to enhance the controller's adaptability for various environments and user needs. The extension could also include a seat for the wheelchair, which is supported by prismatic links along the vertical axis to enable the wheelchair user to reach a certain height.

ORCID

Bouatake Hedstrom
https://orcid.org/0009-0000-7691-7366
Rishi Autar
https://orcid.org/0009-0009-1106-9576
Veisinia Vatikani
https://orcid.org/0009-0004-6163-2076
Sushita Sharma
https://orcid.org/0009-0004-3065-538X
Ronal P. Chand
https://orcid.org/0000-0002-8527-040X
Sandeep A. Kumar
https://orcid.org/0000-0002-6951-4742

References

[1] R. Ye, W. Xu, H. Fu, R. K. Jenamani, V. Nguyen, C. Lu, K. Dimitropoulou and T. Bhattacharjee, Rcareworld: A human-centric simulation world for caregiving robots, in *2022 IEEE/RSJ Int. Conf. Intelligent Robots and Systems (IROS)* (IEEE, 2022), pp. 33–40.

[2] B. Sharma and J. Vanualailai, Multi-tasking of n car-like mobile robots via Lyapunov based approach (9, 2005).

[3] M. Xiloyannis, L. Cappello, K. D. Binh, C. W. Antuvan and L. Masia, Preliminary design and control of a soft exosuit for assisting elbow movements and hand grasping in activities of daily living, *J. Rehabil. Assist. Technol. Eng.* **4** (2017) 2055668316680315, PMID: 31186920.

[4] A. S. Dhanjal and W. Singh, Tools and techniques of assistive technology for hearing impaired people, *2019 Int. Conf. Machine Learning, Big Data, Cloud and Parallel Computing (COMITCon)*, (IEEE, 2019), pp. 205–210.

[5] S. Busaeed, R. Mehmood, I. Katib and J. M. Corchado, Lidsonic for visually impaired: Green machine learning-based assistive smart glasses with smart app and Arduino, *Electronics* **11**(7) (2022) 1076.

[6] T. G. D. P. L. D. X. Sajay Arthanat, Momotaz Begum and N. Zhang, Caregiver perspectives on a smart home-based socially assistive robot for individuals with Alzheimer's disease and related dementia, *Disabil. Rehabil. Assist. Technol.* **15**(7) (2020) 789–798.

[7] C. Liu, Y. Liu, R. Xie, Z. Li, S. Bai and Y. Zhao, The evolution of robotics: Research and application progress of dental implant robotic systems, *Int. J. Oral Sci.* **16**(1) (2024) 28.

[8] E. Martinez-Martin and A. Costa, Assistive technology for elderly care: An overview, *IEEE Access* **9** (2021) 92420–92430.

[9] R. Barros, A. Burlamaqui, S. Azevedo, S. de L. Sa, L. Goncalves and A. da S Burlamaqui, Cardbot — assistive technology for visually impaired in educational robotics: Experiments and results, *IEEE Latin Am. Trans.* **15**(3) (2017) 517–527.

[10] P. Uluer *et al.*, Experience with an affective robot assistant for children with hearing disabilities, *Int. J. Soc. Robot.* **15** (2023) 643–660.

[11] Industry 1.0 to 4.0: 2.3 revolution https://sustainability-success.com/industry-1-0-to-4-0-2-3-revolution/#%Ustry_1.0_to_4.0, Accessed on: 2024-06-06.

[12] E. P. G. Rakasena and L. Herdiman, Electric wheelchair with forward-reverse control using electromyography (EMG) control of arm muscle, *J. Phys. Conf. Ser.* **1450** (2020) 012118.

[13] Q. Huang, Y. Chen, Z. Zhang, S. He, R. Zhang, J. Liu, Y. Zhang, M. Shao and Y. Li, An EOG-based wheelchair robotic arm system for assisting patients with severe spinal cord injuries, *J. Neural Eng.* **16** (2019) 026021.

[14] M. M. Abdulghani, K. M. Al-Aubidy, M. M. Ali and Q. J. Hamarsheh, Wheelchair neuro fuzzy control and tracking system based on voice recognition, *Sensors* **20**(10) (2020) 2872.

[15] B. M. Dicianno, D. M. P. Spaeth, R. A. P. Cooper, S. G. P. Fitzgerald and M. M. Boninger, Advancements in power wheelchair joystick technology: Effects of isometric joysticks and signal conditioning on driving performance, *Am. J. Phys. Med. Rehabil.* **85**(3) (2006) 250.

[16] R. A. Kalantri and D. Chitre, Automatic wheelchair using gesture recognition, *Int. J. Eng. Innov. Technol.* **2**(9) (2013) 216–218.

[17] S. Sahoo and B. Choudhury, Voice-activated wheelchair: An affordable solution for individuals with physical disabilities, *Manag. Sci. Lett.* **13**(3) (2023) 175–192.

[18] M. N. Sahadat, S. Dighe, F. Islam and M. Ghovanloo, An independent tongue-operated assistive system for both access and mobility, *IEEE Sens. J.* **18**(22) (2018) 9401–9409.

[19] M. E. Alam, M. Abdul Kader, U. Hany, R. Arjuman, A. Siddika and M. Z. Islam, A multi-controlled semi-autonomous wheelchair for old and physically challenged people, in *2019 1st Int. Conf. Advances in Science, Engineering and Robotics Technology (ICASERT)*, (IEEE, 2019), pp. 1–6.

[20] S. Kumar, J. Vanualailai and A. Prasad, Assistive technology: Autonomous wheelchair in obstacle-ridden environment, *PeerJ Comput. Sci.* **7** (2021) 1–23.

[21] H.-Y. Ryu, J.-S. Kwon, J.-H. Lim, A.-H. Kim, S.-J. Baek and J.-W. Kim, Development of an autonomous driving smart wheelchair for the physically weak, *Appl. Sci.* **12**(1) (2022) 377.
[22] M. Bellis, History of the wheelchair https://www.thoughtco.com/history-of-the-wheelchair-1992670, Accessed on: 2024-06-06.
[23] E. Blakemore, Wheelchair history: From innovation to independence https://www.nationalgeographic.com/history/article/wheelchair-history-innovation-technology-independence, Accessed on: 2024-06-06.
[24] R. Cooper, T. Corfman, S. Fitzgerald, M. Boninger, D. Spaeth, W. Ammer and J. Arva, Performance assessment of a pushrim-activated power-assisted wheelchair control system, *IEEE Trans. Control Syst. Technol.* **10**(1) (2002) 121–126.
[25] C. Bonneau, History of wheelchairs: Complete timeline & their revolution https://loaids.com/history-of-wheelchairs/, Accessed on: 2024-06-06.
[26] J. Tang, Y. Liu, D. Hu and Z. Zhou, Towards BCI-actuated smart wheelchair system, *BioMed. Eng. OnLine* **17**(1) (2018) 111.
[27] Y. Morales, A. Watanabe, F. Ferreri, J. Even, K. Shinozawa and N. Hagita, Passenger discomfort map for autonomous navigation in a robotic wheelchair, *Robot. Auton. Syst.* **103** (2018) 13–26.
[28] F. Coelho, L. P. Reis, B. M. Faria, A. Oliveira and V. Carvalho, Multimodal intelligent wheelchair interface, in *Trends and Innovations in Information Systems and Technologies*, eds. A. Rocha, H. Adeli, L. P. Reis, S. Costanzo, I. Orovic and F. Moreira (Springer International Publishing, Cham, 2020), pp. 679–689.
[29] K. Banach, M. Malecki, M. Rosol and A. Broniec, Brain computer interface for electric wheelchair based on alpha waves of EEG signal, *Bio-Algorithms Med-Syst.* **17**(3) (2021) 165–172.
[30] N. Farheen, Object detection, localization and navigation strategy for obstacle avoidance applied to autonomous wheelchair driving, Ph.D. thesis (2022).
[31] B. Sharma, Robotic dog for navigation of a rehabilitation wheelchair robot in a highly constrained environment, *PLOS ONE* **19** (2024) 1–21.
[32] A. Naderolasli, K. Shojaei and A. Chatraei, Terminal sliding-mode disturbance observer-based finite-time adaptive-neural formation control of autonomous surface vessels under output constraints, *Robotica* **41**(1) (2023) 236–258.
[33] A. Naderolasli, K. Shojaei and A. Chatraei, Fixed-time multilayer neural network-based leader–follower formation control of autonomous surface vessels with limited field-of-view sensors and saturated actuators, *Neural Comput. Appl.* **37**(21) (2024) 16071–16091.
[34] A. Naderolasli, K. Shojaei and A. Chatraei, Platoon formation control of autonomous underwater vehicles under LOS range and orientation angles constraints, *Ocean Eng.* **271** (2023) 113674.
[35] A. Naderolasli, Indirect self-tuning controller for a two degree of freedom tracker model, *Int. J. Veh. Auton. Syst.* **16**(1) (2021) 15–37.
[36] J. Raj, K. Raghuwaiya, R. Havea and J. Vanualailai, Autonomous control of multiple quadrotors for collision-free navigation, *IET Control Theory Appl.* **17**(7) (2023) 868–895.
[37] J. Vanualailai, S. ichi Nakagiri and J.-H. Ha, Collision avoidance in a two-point system via Liapunov's second method, *Math. Comput. Simul.* **39**(1) (1995) 125–141.
[38] J. Ha and J. Vanualailai, A collision avoidance control problem for moving objects and a robot arm, *J. Korean Math. Soc.* **35**(1) (1998) 135–148.
[39] A. Prasad, B. Sharma and J. Vanualailai, Motion camouflage for point-mass robots using a Lyapunov-based control scheme, in *2019 4th Int. Conf. Control and Robotics Engineering (ICCRE)*, (IEEE, 2019), pp. 7–11.
[40] J. Raj, K. Raghuwaiya, J. Vanualailai and B. Sharma, Navigation of car-like robots in three-dimensional space, in *2018 5th Asia-Pacific World Congress on Computer Science and Engineering (APWC on CSE)*, (IEEE, 2018), pp. 271–275.
[41] D. Kumar, J. Raj, K. Raghuwaiya and J. Vanualailai, Autonomous UAV landing on mobile platforms, *2021 IEEE Asia-Pacific Conf. Computer Science and Data Engineering (CSDE)*, (IEEE, 2021), pp. 1–6.
[42] R. Chand, K. Raghuwaiya, J. Vanualailai and J. Raj, Leader-follower based low-degree formation control of fixed-wing unmanned aerial vehicles in 3D, in *Proceedings of Third Int. Conf. Advances in Computer Engineering and Communication Systems*, eds. A. B. Reddy, S. Nagini, V. E. Balas and K. S. Raju (Springer Nature Singapore, Singapore, 2023), pp. 101–118.
[43] J. Vanualailai, A. Sharan and B. Sharma, A swarm model for planar formations of multiple autonomous unmanned aerial vehicles, in *2013 IEEE Int. Symp. Intelligent Control (ISIC)*, (IEEE, 2013), pp. 206–211.
[44] B. Sharma, J. Vanualailai and A. Prasad, Formation control of a swarm of mobile manipulators, *Rocky Mt. J. Math.* **41**(3) (2011) 909–940.
[45] R. Chand, B. Sharma and S. A. Kumar, Collaborative mobile manipulators for distributed task execution in smart city applications, *IEEE Access* **13** (2025) 143925–143938.
[46] B. Siciliano, L. Sciavicco, L. Villani and G. Oriolo, in *Robotics: Modelling, Planning and Control*, 1st edn. (Springer, London, 2009).
[47] H. Grewal, A. Matthews, R. Tea and K. George, LIDAR-based autonomous wheelchair, in *2017 IEEE Sensors Applications Symp. (SAS)*, (IEEE, 2017), pp. 1–6.
[48] G. Foresi, A. Freddi, A. Monteriu, D. Ortenzi and D. P. Pagnotta, Improving mobility and autonomy of disabled users via cooperation of assistive robots, in *2018 IEEE Int. Conf. Consumer Electronics (ICCE)*, (IEEE, 2018), pp. 1–2.
[49] A. Jayakody, A. Nawarathna, I. Wijesinghe, S. Liyanage and J. Dissanayake, Smart wheelchair to facilitate disabled individuals, in *2019 Int. Conf. Advancements in Computing (ICAC)*, (IEEE, 2019), pp. 249–254.

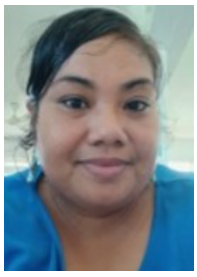

Bouatake Hedstrom received her Bachelor of Science degree, majoring in Mathematics and Physics, from The University of the South Pacific (USP) in 2012, followed by a Graduate Certificate in Education in 2017 from the same institution. Since 2013, she has been teaching secondary school Mathematics and Physics. Currently, she is pursuing postgraduate studies in Mathematics at USP. A passionate advocate for her Banaban community, Bouatake is dedicated to improving educational opportunities for youth. She aspires to become one of the first women from her community to achieve success in the field of Mathematics.

Rishi Autar earned his Bachelor of Science degree, majoring in Mathematics and Physics, along with a Graduate Certificate in Education from USP in 2018. He is currently pursuing postgraduate studies in Mathematics at USP. Since 2018, he has been working as a secondary school teacher for Mathematics and Physics under the Ministry of Education. With over 7 years of teaching experience, Rishi has participated in numerous professional development courses, refining his teaching methods and incorporating engaging activities that cater to diverse learning styles.

Veisinia Vatikani is currently a full time teacher in one of the Free Wesleyan schools in Tonga teaching Chemistry and Mathematics for both junior and senior levels. She is also a part-time student at USP, pursuing a Postgraduate Diploma in the field of Mathematics.

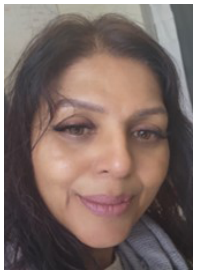

Sushita Sharma is a dedicated educator with an MSc in Mathematics, currently pursuing a PhD in the same field. She has 6 years of experience teaching Mathematics and Physics at local schools in Fiji before joining International School Suva (ISS) as Head of Mathematics. At ISS, she taught the International Baccalaureate Diploma Program for 15 years and continues to serve as a moderator for Internal Assessments and Final Examinations. She has also contributed to the implementation of the Australian Curriculum (ACT). Presently, she works as a teaching assistant in the Mathematics and Statistics discipline at USP.

Ronal Pranil Chand is a Lecturer in Mathematics at Fiji National University (FNU). He holds a Postgraduate Diploma and a Master of Science in Mathematics. Currently, he is pursuing Ph.D. in Mathematics from FNU. His research focuses on developing algorithms and mathematical models for motion control and planning for robotic systems.

Sandeep Ameet Kumar received his BScGCE, MSc and PhD degrees from USP in 2010, 2014 and 2024, respectively. Currently, he is serving USP as a Lecturer in Mathematics. His research focuses on motion planning and control in robotics, inspired by nature. He specializes in designing nonlinear, time-invariant, continuous, stabilizing algorithms using the Lyapunov-based control scheme for complex mechanical systems in constrained environments. His work, primarily theoretical, has applications in autonomous assistive wheelchairs, UAV swarms for EEZ surveillance, and robotic manipulators. He is also investigating the applicability of other classical, heuristic, and hybrids which could provide better problem-based solutions in his research areas.